DOI: 10.11134/btp.4.2025.16

UDC: 576.31, 576.88

Original Article

GENERATION OF MITOCHONDRIA-DEPLETED (RHO0) MDA-MB-231 CELLS AND CHARACTERIZATION

B. Kenzhetay[1], A. Dildabek[2], A.N. Burska[3]*

[1]Department of Biomedical Sciences, School of Medicine, Nazarbayev University, Astana, Kazakhstan;
[2]Department of Biology, School of Sciences and Humanities, Nazarbayev University, Astana, Kazakhstan;
[3]National Laboratory of Astana, Nazarbayev University, Astana, Kazakhstan
Corresponding author: agata.burska@nu.edu.kz

ABSTRACT

Mitochondrial depletion models are indispensable for understanding the role of mitochondrial function in cancer metabolism and signaling. However, traditional approaches such as ethidium bromide or nucleoside analogue treatments often induce nuclear mutagenesis and incomplete mitochondrial clearance. Here, we present a controlled and reproducible strategy to generate mitochondria-depleted (Rho0) MDA-MB-231 breast cancer cells through enforced mitophagy driven by Parkin overexpression.

Stable Parkin-overexpressing (PKN OE) cells were established via lentiviral transduction and subjected to repetitive mitochondrial depolarization using carbonyl cyanide m-chlorophenyl hydrazone (CCCP) in uridine- and pyruvate-supplemented medium. This approach triggered sustained PINK1–Parkin pathway activation, resulting in progressive mitochondrial clearance. Quantitative PCR confirmed >95% reduction in mitochondrial DNA (*ND1*) copy number, while immunoblotting showed loss of TOMM20 and VDAC1. Confocal microscopy with MitoTracker Deep Red revealed a near-complete absence of the mitochondrial network. Despite mitochondrial depletion, cells maintained viability and displayed metabolic adaptation, with no significant change in basal ATP or lactate levels. Cell proliferation and cell cycle analyses demonstrated slower growth and G1 accumulation in Rho0 cells, reflecting impaired bioenergetic support for DNA synthesis.

This Parkin-mediated mitophagy model provides a physiologically relevant and non-mutagenic platform for studying mitochondrial dysfunction, metabolic plasticity, and retrograde signaling in triple-negative breast cancer. It offers a versatile tool for future investigations into therapeutic resistance, mitochondrial translation disorders, and mitochondrial-nuclear communication in tumor progression.

Key words: Mitochondrial depletion; Rho0 cells; *Parkin* overexpression; enforced mitophagy; CCCP; MDA-MB-231; triple-negative breast cancer; mitochondrial DNA loss; bioenergetic adaptation; mitophagy model; mitochondrial dysfunction; cell cycle regulation; metabolic reprogramming.

INTRODUCTION

Among the various organelles in eukaryotic cells, mitochondria are unique not only because of their central role in energy production but also because they contain their own genetic material. Human mitochondrial DNA (mtDNA) is a 16.6-kb double-stranded, covalently closed circular genome encoding 13 polypeptides essential for the oxidative phosphorylation (OXPHOS) system, along with two ribosomal RNAs (rRNAs) and 22 transfer RNAs (tRNAs) [1]. These mitochondrially encoded proteins are integral subunits of the respiratory chain/electron transport chain (ETC), and their expression is crucial for ATP generation, redox balance, and the regulation of cell survival and death pathways [2]. The unique uniparental inheritance pattern of mitochondria, being maternally transmitted, and their semi-autonomous replication make them particularly intriguing for studies on cellular metabolism and disease. Loss or depletion of mtDNA profoundly affects these processes, forcing cells to rely on compensatory mechanisms such as glycolysis to sustain energy production and maintain viability.

Mitochondria-depleted (Rho0) cell lines, which lack functional mitochondrial DNA (mtDNA), are powerful tools for studying the contributions of mitochondria to cellular physiology. They allow us to directly assess how mitochondrial metabolism influences proliferation, differentiation, and stress responses. These Rho0 cells are also indispensable for investigating retrograde signaling, a process where mitochondria communicate functional status to the nucleus, triggering adaptive gene expression programs in response to mitochondrial stress [3–5]. Furthermore, Rho0 cells facilitate the generation of cytoplasmic hybrid (cybrid) lines, in which isolated mitochondria from one donor are fused with a Rho0 recipient cell containing a nucleus. Using this cellular model enables precise investigation of mitochondrial-nuclear interactions under a known and controlled nuclear background [6]. Experiments with these cells have greatly advanced the understanding of mitochondrial biology, aging, and disease pathogenesis. Rho0 models also enable scientists to investigate how cells adapt metabolically and structurally to the complete absence of mitochondrial function, revealing compensatory pathways that may contribute to survival under stress conditions.

Historically, mitochondrial depletion has been achieved through long-term exposure to ethidium bromide (EtBr), a DNA intercalating agent. EtBr preferentially inhibits mtDNA replication because mitochondrial DNA has limited repair capacity, whereas nuclear DNA is less affected by this agent because of robust repair mechanisms [7, 8]. Despite its effectiveness, EtBr has significant drawbacks. Generating Rho0 cells using EtBr is very slow, often requiring several weeks/months of continuous culture to achieve complete mtDNA loss. Additionally, EtBr is mutagenic and can induce nuclear genomic instability, which complicates downstream analyses [9, 10]. Alternative chemical approaches, including nucleoside ana-

DOI: 10.11134/btp.4.2025.16

logs such as 2′,3′-dideoxycytidine (ddC) and 2′-C-methyladenosine (2′-C-MeA), selectively inhibit mtDNA replication or transcription, improving specificity relative to EtBr. Enzymatic strategies, such as mitochondrially targeted restriction endonucleases (e.g., EcoRI) or the expression of dominant-negative DNA polymerase γ (*POLG*), have also been explored [11, 12]. Nevertheless, a fundamental limitation remains: even if the mitochondrial DNA (mtDNA) is gone or nonfunctional, the mitochondria themselves still exist as structures in the cell. Although they cannot carry out normal mitochondrial functions like ATP production through oxidative phosphorylation, they can still influence non-respiratory mitochondrial functions, such as calcium buffering and local protein interactions, cellular signaling and morphology, potentially confounding experimental results.

The role of mitochondria is particularly critical in cancer biology. In aggressive cancers, such as triple-negative breast cancer (TNBC), the MDA-MB-231 cell line, mitochondria support not only energy production but also biosynthetic metabolism, redox homeostasis, and regulation of apoptosis. Cancer cells exploit mitochondrial functions to survive in hypoxic and nutrient-poor microenvironments, resist chemotherapeutic agents, and adapt to metabolic stress. Understanding how TNBC cells adapt to mitochondrial loss can shed light on metabolic vulnerabilities that could be targeted therapeutically, especially in tumors that exhibit resistance to conventional chemotherapies [13, 14]. Models that enable complete removal of mitochondria provide a unique opportunity to study compensatory metabolic pathways, revealing potential points of intervention in aggressive cancers. By eliminating the confounding effects of residual mitochondria, Rho0 models allow for more precise interrogation of metabolic and signaling dependencies, offering insights that may inform novel treatment strategies.

A physiological and promising method to generate mitochondria-depleted cells is Parkin-induced mitophagy. Parkin, encoded by the *PARK2* gene, is an E3 ubiquitin ligase that selectively localizes to depolarized or damaged mitochondria. The recruitment of Parkin to mitochondria is tightly regulated by PINK1, a kinase that accumulates on the outer membrane of depolarized mitochondria. PINK1 phosphorylates both ubiquitin and Parkin, activating its E3 ligase function and promoting the ubiquitination of outer membrane proteins [15-17]. These ubiquitinated mitochondria are then recognized by autophagy receptors, including p62/SQSTM1, NDP52, and optineurin, which link the organelle to the autophagy machinery for lysosomal degradation. This process mirrors physiological mitochondrial quality control, maintaining cellular homeostasis by removing damaged organelles and preventing excessive accumulation of reactive oxygen species. By sustaining Parkin activation under conditions that suppress mitochondrial biogenesis, cells undergo progressive clearance of the mitochondrial network, ultimately achieving complete depletion of mtDNA and the removal of mitochondrial structures. This approach not only avoids the mutagenic effects associated with chemical methods but also produces cells that are both bioenergetically and structurally devoid of mitochondria, accurately reflecting a true Rho0 phenotype.

In the present study, we applied Parkin-mediated mitophagy to generate Rho0 MDA-MB-231 cells. Culture conditions and Parkin expression levels were optimized to ensure efficient mitochondrial clearance within three weeks. The resulting clones were validated using multiple complementary approaches, including quantitative PCR for mtDNA depletion, immunoblotting to confirm the loss of mitochondrial respiratory proteins, and functional assays demonstrating the absence of oxidative phosphorylation. These Rho0 cells provide a physiologically relevant and reproducible model for exploring mitochondrial contributions to proliferation, metabolic adaptation, and cellular signaling in TNBC.

Overall, this approach establishes a robust platform for interrogating the dependence of TNBC cells on mitochondrial function and metabolic flexibility. By combining the physiological specificity of Parkin-induced mitophagy with rigorous validation, this study provides a safe, efficient, and reproducible strategy for generating mitochondria-depleted cells. The Rho0 MDA-MB-231 model has broad applications in cancer research, including studies on metabolic rewiring, retrograde signaling, and resistance to therapy, providing a foundation for future therapeutic exploration.

Materials and Methods

Cell Culture: The human triple-negative breast cancer cell line MDA-MB-231 (ATCC, Cat. No. HTB-26) was cultured in high-glucose Dulbecco's Modified Eagle Medium F-12 (DMEM-F12, 17.5g/L glucose, Gibco, Cat. No. 12500096) supplemented with 10% fetal bovine serum (Capricorn, Cat. No. FBS-HI-11A), 100 U/mL penicillin, and 100 µg/mL streptomycin (Thermo Fisher Scientific, 15140122). Cells were maintained at 37°C in a humidified 5% CO_2 atmosphere. For the generation and maintenance of mitochondrial DNA-depleted (Rho0) cells, the medium was supplemented with 50 µg/mL uridine (Sigma-Aldrich, Cat. No. U3750-25G) and 100 µg/mL sodium pyruvate (Sigma Aldrich, Cat. No. P5280). These supplements were essential to support pyrimidine nucleotide synthesis and maintain cell viability in the absence of functional oxidative phosphorylation.

Generation of Parkin-Overexpressing MDA-MB-231 Cells

The Parkin plasmid pMXs-IP HA-Parkin (Addgene, Cat No. 38248) containing human *PARK2* cDNA with an N-terminal HA tag was overexpressed from the aforementioned vector. Lentiviral particles were generated in HEK293T cells (ATCC, Cat. No. CRL-3216) by co-transfection with the packaging plasmid pCL-Ampho (NOVUS Biologicals, Cat. No. NBP2-29541) using Polyethylenimine (Thermo Fisher Scientific, Cat. No. 043896.01) according to the manufacturer's instructions. Viral supernatants were collected 48 hours post-transfection, centrifuged, and used immediately for cell transduction. MDA-MB-231 cells were transduced with the HA-Parkin lentivirus in the presence of 8 µg/mL polybrene (Sigma Aldrich, Cat. No. TR-1003) to enhance infection efficiency. Stable cell populations were selected with 10 µg/mL puromycin (Thermo Fisher Scientific, Cat. No. A1113803) for 48 hours. Expression of HA-Parkin was confirmed by Western blotting using an anti-HA antibody (HA-Tag (C29F4) Rabbit mAb, #3724, Cell Signaling Technology). Parental MDA-MB-231 cells transduced with an empty vector served as controls.

Induction of Mitophagy and Mitochondrial Depletion

DOI: 10.11134/btp.4.2025.16

To induce widespread mitophagy and progressive mitochondrial depletion, we adapted the protocol of Correia-Melo et al., 2017 [18]. Parkin-overexpressing MDA-MB-cells were treated with carbonyl cyanide m-chlorophenyl hydrazone (CCCP, Abcam, Cat. No. ab141229), a protonophore that collapses the mitochondrial membrane potential (ΔΨm). Cells were exposed to 7.5–10 μM CCCP for 48 hours, with fresh CCCP added every 12 hours to maintain depolarization. The culture media was replaced with DMEM supplemented with uridine (50 μg/mL) and sodium pyruvate (100 μg/mL) to support nucleotide biosynthesis and ensure viability during mitochondrial clearance. Following the 48-hour CCCP treatment, cells were allowed to recover for an additional 24-48 hours in the same supplemented medium to permit complete mitophagic flux and adaptation.

Quantification of mtDNA Copy Number (mtDNA CN)

Total DNA was isolated using the PureLink™ Genomic DNA Mini Kit (Thermo Fisher Scientific, Cat. No. K182002) according to the manufacturer's instructions. Quantitative PCR (qPCR) was performed using primers targeting the mitochondrial NADH dehydrogenase 1 (*ND1)* gene and the nuclear hydroxymethylbilane synthase (*HMBS)*.

Primer sequences:

ND1 forward: GGCTATATACAACTACGCAAAGGC

ND1 reverse: GGTAGATGTGGCGGGTTTTAGG

HMBS forward: ACGGCTCAGATAGCATACAAGAG

HMBS reverse: GTTACGAGCAGTGATGCCTACC

Reactions were carried out using Power SYBR™ Green PCR Master Mix (Applied Biosystems, Cat. No. 4309155) on a QuantStudio™ 7 Real-Time PCR System (Thermo Fisher Scientific, Cat. No. 4485701). The relative mtDNA copy number was calculated by the ΔΔCt method. Rho0 cells were defined as those exhibiting <1% mtDNA content relative to parental controls over at least two consecutive passages.

Western Blotting

Cells were lysed in RIPA buffer supplemented with protease and phosphatase inhibitors (Halt™ Protease Inhibitor Cocktail (100X), Thermo Fisher Scientific, Cat. No. 78429). Equal amounts of protein (20–30 μg) were separated on 10–12% SDS-PAGE gels and transferred to PVDF membranes (BioRad, Cat. No. 1620177). Membranes were blocked in 5% non-fat milk for 1 hour and probed overnight at 4°C with the following primary antibodies: Anti-HA tag (HA-Tag (C29F4) Rabbit mAb, #3724, CST) at 1:2000 dilution; Anti-beta-tubulin (loading control; β-Tubulin (9F3) Rabbit mAb #2128, CST) at 1:1000 dilution; VDAC1 (VDAC (D73D12) Rabbit mAb #4661, CST) at 1:1000 dilution; TOMM20 (Abcam, Cat. No. AB186735) at 1:1000 dilution. After incubation with HRP-conjugated secondary antibodies (CST, Cat. No. #7074) at a 1:20000 dilution, detection was performed using ECL substrate (CST, Cat. No. 6883) and imaged on a ChemiDoc™ MP Imaging System (Bio-Rad).

Microscopic Observation of Cell and Mitochondria Morphology

Cells were seeded in 6-well plates and allowed to adhere for 24 hours before treatment. Morphological changes were visualized by phase-contrast microscopy using a Primovert (Zeiss) microscope equipped with 10×, 20×, and 40× objectives. Images were captured using Zeiss Zen software (version 3.7). For confocal imaging, cells were seeded at a density of 150,000 cells per 35mm confocal dish and allowed to adhere for 24 h. Following adherence, cells were stained with 50nM MitoTracker Deep Red (MTDR) (mitochondrial staining, Thermo Fisher Scientific, Cat. No. M22426) and 1:1500 Hoechst (nuclear staining, Thermo Fisher Scientific, Cat. No. 33342). Imaging was performed using a Spinning Disk Cell Observer (Carl Zeiss) microscope and imaged via MetaMorph software (Gataca Systems, MM 7.10.5), and appropriate filter sets were used to capture Hoechst (ex/em ~350/461 nm) and MTDR (ex/em ~644/665 nm) signal.

Growth and Metabolic Assays

Growth rates of MDA-MB-231 and Rho0 cells were assessed using the CellTiter 96® AQueous One Solution Cell Proliferation Assay (MTS) (Promega, Cat. No. G3582) at 24 and 48 hours. Cells were cultured in either standard DMEM-F12 or uridine/pyruvate-supplemented medium. Rho0 clones were expected to exhibit growth arrest in non-supplemented media, confirming functional mitochondrial depletion. Lactate concentration in culture media was quantified using the Lactate-Glo™ Assay (Promega, Cat. No. J5021), while ATP levels were measured with the ATP Determination Kit (Thermo Fisher Scientific, Cat. No. A22066) according to the manufacturer's instructions.

Real-Time Cell Proliferation Analysis (xCELLigence RTCA)

Real-time monitoring of cell proliferation was performed using the xCELLigence Real-Time Cell Analysis (RTCA) DP system (Agilent Technologies, USA), which measures electrical impedance across microelectrodes integrated at the bottom of each well of a specialized E-plate (Cat. No. E-plate 16). The impedance is expressed as a dimensionless parameter known as the cell index (CI), which reflects cell number, viability, and adhesion dynamics. Briefly, E-16 plates were preconditioned with 100 μL of the respective culture medium: DMEM-F12 for parental cells and uridine/pyruvate-supplemented DMEM for Rho0 cells. The E-plate was then left to equilibrate for 30 min inside the RTCA station. Following baseline impedance measurement, 10,000 MDA-MB-231 or Rho0 cells per well were seeded in 200 μL of respective media and monitored for up to 96 hours. The RTCA station was housed within a standard CO_2 incubator (37 °C, 5% CO_2). Cell impedance was automatically recorded every 15 minutes for up to 96 hours using the RTCA software version 2.1.0 (Agilent). Proliferation kinetics were expressed as cell index (CI) vs. time plots. Growth rates were compared between parental and Rho0 MDA-MB-231 cells. Data were analyzed using RTCA Data Analysis Software (Agilent). Each experiment was performed in triplicate and repeated independently at least three times.

Cell Cycle Analysis by Flow Cytometry

Cell cycle distribution of parental and mitochondria-depleted (Rho0) MDA-MB-231 cells was assessed by propidium iodide (PI) staining and analyzed using an Attune NxT Flow Cytometer (Thermo Fisher Scientific, USA). Cells were seeded in 6-well plates at a density of 1.5 × 10 ^5 cells per well and cultured under standard conditions (37°C, 5% CO_2) for 24 hours to allow for attachment. After experimen-

DOI: 10.11134/btp.4.2025.16

tal treatment or the indicated incubation periods (24 h and 48 h), both adherent and floating cells were harvested by gentle trypsinization, pooled to avoid cell loss, and washed twice with ice-cold phosphate-buffered saline (PBS, pH 7.4). Cells were fixed by slow dropwise addition of ice-cold 70% ethanol while gently vortexing to prevent clumping. Fixed cells were stored at 4°C for at least 2 hours or overnight to ensure adequate permeabilization of the nuclear membrane. Before staining, samples were centrifuged at 500 × g for 5 minutes at 4°C and washed twice with PBS to remove residual ethanol. Cell pellets were resuspended in 500 µL of PI/RNase staining buffer containing 50 µg/mL propidium iodide (Thermo Fisher Scientific, Cat. No. P3566) and 50 µg/mL RNase A (Thermo Fisher Scientific, Cat. No. EN0531) in PBS. Samples were incubated at 37°C for 30 minutes in the dark to allow uniform staining and complete RNA degradation. Stained samples were acquired on the Attune NxT Flow Cytometer equipped with a 488 nm blue laser. PI fluorescence was collected using the BL2 (585/40 nm) emission filter. A minimum of 10,000 single-cell events were recorded for each sample. Cell debris, doublets, and aggregates were excluded by sequential gating using forward scatter (FSC-A vs FSC-H) and side scatter (SSC-A) parameters. Cell cycle phase distribution (G_0/G_1, S, and G_2/M) was determined using FlowJo™ Software v10.0.7 (BD Biosciences), and the proportions of cells in each phase were automatically calculated.

Statistical Analysis

All experiments were performed in at least three independent biological replicates. Data are presented as mean ± standard deviation (SD). Statistical comparisons between groups were conducted using unpaired two-tailed Student's *t*-tests or one-way ANOVA where appropriate. A p-value < 0.05 was considered statistically significant. Graphs were generated using GraphPad Prism v9.0 (GraphPad Software, USA).

RESULTS

1. Generation of Parkin-Overexpressing MDA-MB-231 Cells

To enable controlled induction of mitophagy in MDA-MB-231 cells, we first established a stable Parkin-overexpressing cell line. Parkin, encoded by the *PARK2* gene, is an E3 ubiquitin ligase recruited to depolarized mitochondria, where it ubiquitinates outer membrane proteins and marks them for recognition by the autophagy machinery. Using this natural quality-control pathway, we aimed to create a system that selectively and progressively clears mitochondria in a physiologically relevant way, thereby avoiding the rapid or potentially mutagenic effects associated with conventional chemical depletion methods.

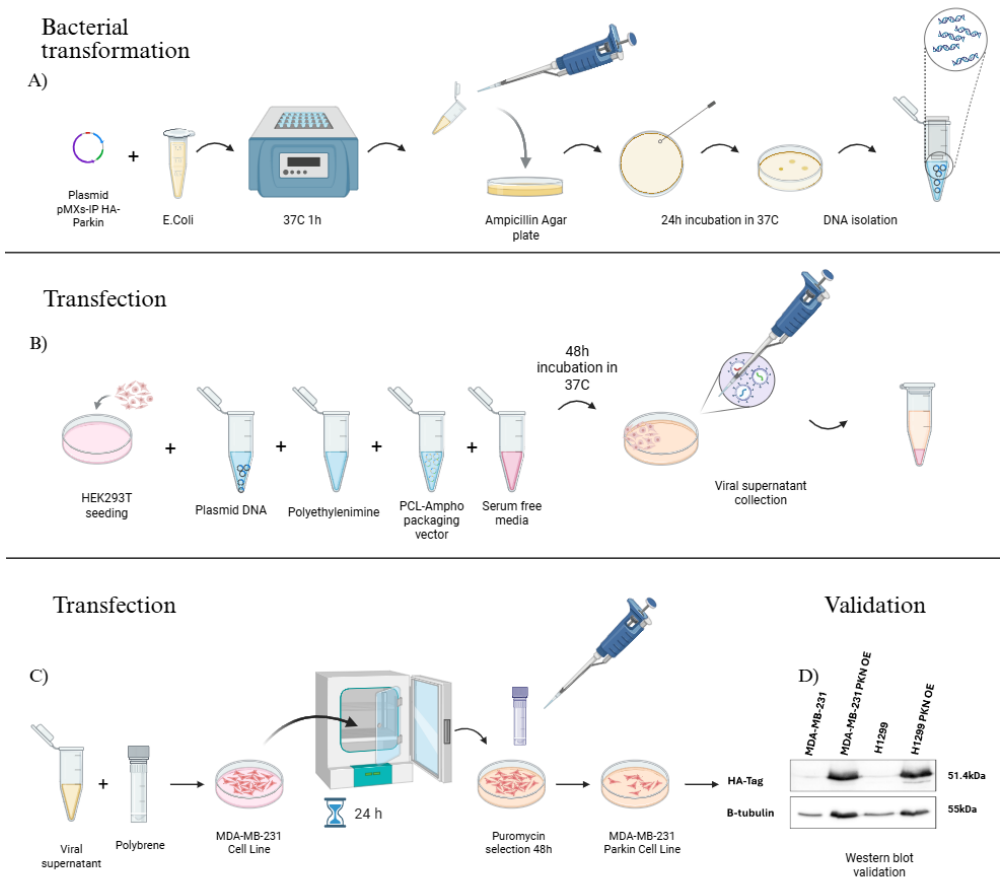

Figure 1. Schematic workflow for the generation of Parkin-overexpressing MDA-MB-231 cells. A) Bacterial transformation for amplification of the HA-Parkin plasmid. This step ensures sufficient plasmid DNA is available for subsequent viral production. B) Transfection of 293T packaging cells to generate lentiviral particles carrying the HA-Parkin construct. Efficient viral production is critical for successful transduction of target cells. C) Transduction of MDA-MB-231 cells with the lentiviral vector, followed by selection of stable populations under antibiotic pressure. D) Western blot validation of successful Parkin OE was done using antibodies against HA-Parkin tag in selected clones of MDA MB 231 and H1299 cell lines, establishing a robust model for subsequent mitophagy induction experiments.

DOI: 10.11134/btp.4.2025.16

MDA-MB-231 cells were transduced with a lentiviral vector encoding HA-tagged *PARK2*, and stable populations were selected under antibiotic pressure. Expression of HA-Parkin was verified by Western blotting, which showed a strong HA-specific band in transduced cells, while parental controls displayed no detectable expression. This confirmed the successful establishment of Parkin OE cells. The modified cells retained normal morphology and proliferative capacity, indicating that Parkin overexpression alone did not compromise cell viability or induce cellular stress.

A schematic overview of the workflow is presented in Figure 1, illustrating the main stages of the process: bacterial transformation and plasmid amplification, transfection of 293T cells for lentiviral particle production, transduction of MDA-MB-231 cells, and validation of HA-Parkin expression.

Establishing Parkin OE MDA-MB-231 cells provides a robust foundation for subsequent induction of mitophagy and for investigating mitochondrial dynamics, bioenergetic adaptation, and cellular responses to mitochondrial loss in triple-negative breast cancer cells [19].

2. Induction of Mitochondrial Depletion in Parkin-Overexpressing Cells

To trigger widespread mitophagy in the established Parkin OE MDA-MB-231 cells, we adapted the protocol described by Correia-Melo et al. [18], which relies on repetitive mitochondrial depolarization using carbonyl cyanide m-chlorophenyl hydrazone (CCCP). CCCP functions as a protonophore and uncoupler of oxidative phosphorylation, collapsing the mitochondrial membrane potential (MMP) and inducing morphological swelling and dysfunction of mitochondria. These changes promote the accumulation of PINK1 on the outer mitochondrial membrane, which in turn recruits and activates Parkin, initiating ubiquitination of outer membrane proteins and their recognition by the autophagy machinery.

In our experiments, Parkin OE MDA-MB-231 cells were exposed to CCCP in repetitive cycles over a 48-hour period to achieve progressive mitochondrial depolarization and clearance (Fig 2). Treatments were applied upon media change, using DMEM supplemented with uridine and pyruvate to support cell viability during mitochondrial depletion. Uridine supplementation is particularly important because it provides a source of pyrimidine nucleotides, enabling cells to continue synthesizing nucleic acids in the absence of mitochondrial function, while pyruvate supports energy metabolism via glycolysis. Based on cell line optimization, 7.5 μM CCCP was re-administered every 12 hours to maintain depolarization and sustain mitophagic activity.

This cyclic exposure resulted in efficient recruitment of Parkin to mitochondria, as evidenced by the loss of mtDNA, disruption of mitochondrial structural integrity, and reduction in mitochondrial protein markers in subsequent analyses. Importantly, the treatment regimen was tolerated, and overall cell viability remained acceptable, although some cell death was observed after the first two doses of CCCP.

This approach allowed the generation of a population of cells with severely reduced mitochondrial content, suitable for subsequent analyses of mtDNA depletion, metabolic adaptation, and cellular function in the absence of functional mitochondria.

3. Validation of Mitochondrial Depletion in MDA-MB-231 Rho0 Cells

To verify that Parkin-induced mitophagy successfully generated mitochondria-depleted (Rho0) MDA-MB-231 cells, we performed a combination of molecular, imaging, and biochemical assays (Fig 3). Quantitative PCR analysis of mitochondrial DNA (mtDNA) revealed a pronounced and consistent reduction in copy number compared with the parental cell line (Fig. 3A). Using *ND1* as a mitochondrial gene marker and *HMBS* as a nuclear reference, we observed that mtDNA levels in Rho0 cells were reduced by more than 95%, indicating near-complete elimination of the mitochondrial genome.

To assess mitochondrial content at the cellular level, we next employed confocal fluorescence microscopy using MitoTracker Deep Red (MTDR) to visualize active mitochondria. Parental MDA-MB-231 cells displayed an extensive filamentous and reticular mitochondrial network distributed throughout the cytoplasm, producing a strong and continuous MTDR signal. In contrast, Rho0 cells exhibited a very faint, punctate signal with occasional small fluorescent remnants visible near the perinuclear region (Fig 3C). These puncta most likely represent non-functional mitochondrial remnants or lysosomal structures undergoing final stages of degradation rather than intact organelles. The marked reduction in fluorescent intensity across the cell population confirmed that the majority of mitochondria were eliminated following sustained Parkin activation.

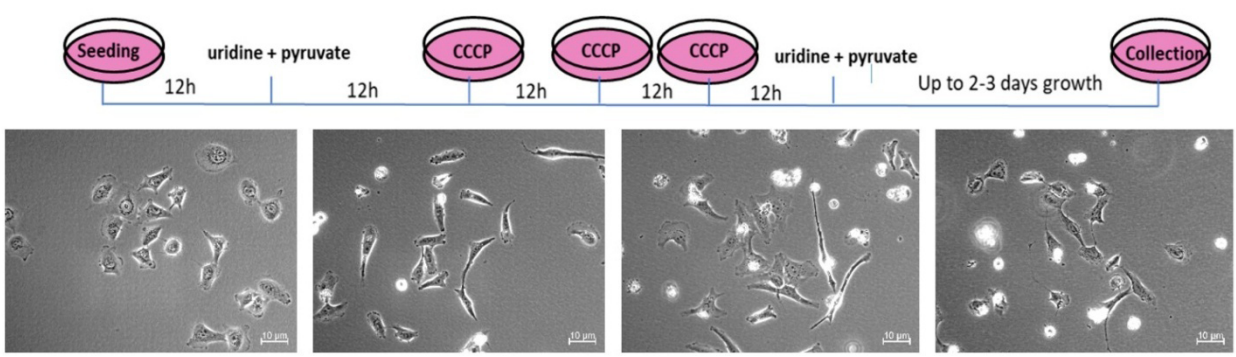

Figure 2. Induction of widespread mitophagy in Parkin-overexpressing cells. Schematic representation of the CCCP-based protocol used to induce mitochondrial depletion in PKN OE MDA-MB-231 cells. Repetitive CCCP treatment every 12 hours over a 48-hour period triggers mitochondrial depolarization and Parkin-mediated mitophagy. Below representative images illustrating mitochondrial depolarization and morphological changes following CCCP treatment.

DOI: 10.11134/btp.4.2025.16

This depletion remained stable during subsequent passages. Monitoring mtDNA copy number across multiple culture cycles by qPCR (Fig. 3B) revealed a gradual but steady decline in residual mtDNA, consistent with ongoing mitophagic activity and progressive adaptation of cells to a mitochondria-deficient state. Over approximately four consecutive passages, mtDNA copy number dropped to below 1% of parental levels and eventually became nearly undetectable. These results indicate that any remaining mitochondrial DNA or nucleoids were continuously cleared through sustained Parkin-mediated mitophagy, leading to the establishment of a stable Rho0 population.

Immunoblotting further validated these findings. Western blot analysis revealed the complete absence of mitochondrial outer membrane proteins TOMM20 and VDAC1 in Rho0 cells, whereas both were strongly expressed in parental MDA-MB-231 controls (Fig 3 D, E). The loss of these markers indicates a near-total absence of mitochondrial structures and confirms successful execution of Parkin-mediated mitophagy.

These biochemical results were in full agreement with qPCR and confocal data, collectively indicating that mitochondria had been almost entirely removed from the cytoplasm. Together, these findings demonstrate that sustained Parkin overexpression effectively triggers mitophagic removal of mitochondria in MDA-MB-231 cells, leading to stable generation of Rho0 clones within approximately one week. The resulting cells show a consistent absence of mtDNA, mitochondrial proteins, and mitochondrial structure, confirming the depletion. This Parkin-based strategy provides a reliable, physiologically relevant, and less genotoxic alternative to traditional chemical approaches such as ethidium bromide or ddC treatment for generating mitochondria-deficient models of triple-negative breast cancer.

4. Cell Proliferation and Cell Cycle Analysis in Parental and Rho0 MDA-MB-231 Cells

To evaluate the functional consequences of mitochondrial depletion on cell growth, proliferation of parental and Rho0 MDA-MB-231 cells was continuously monitored using the xCELLigence Real-Time Cell Analysis (RTCA) system over approximately 55 hours (excluding adhesion time). Cell index values, reflecting cell adherence and proliferation, were recorded and plotted over time. Parental MDA-MB-231 cells (green) displayed a steady and continuous increase in cell index, indicative of robust proliferative capacity. In contrast, Rho0 cells (magenta), lacking functional mitochondrial DNA, exhibited markedly reduced growth, with a consistently lower cell index that plateaued at later time points. These results indicate that the absence of mitochondria significantly limits the proliferative potential of MDA-MB-231 cells (Fig 4).

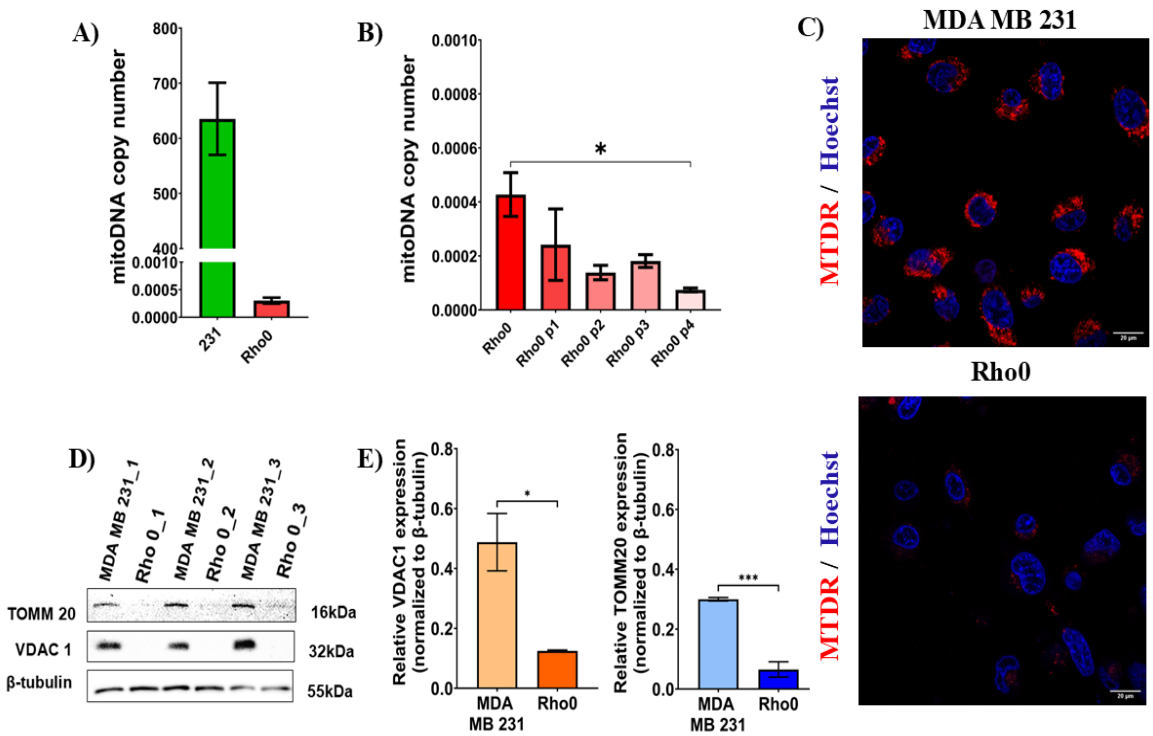

Figure 3. Validation of mitochondrial depletion in MDA-MB-231 Rho0 cells.

A) Quantification of mitochondrial DNA (mtDNA) copy number by qPCR using *ND1* as a mitochondrial marker and *HMBS* as a nuclear reference gene. Rho0 MDA-MB-231 cells showed a near-complete loss of mtDNA compared to parental controls, confirming efficient depletion. B) mtDNA copy number measured across consecutive passages of Rho0 cells revealed a progressive decline, reflecting ongoing mitophagy and cellular adaptation to mitochondrial loss.

C) Confocal fluorescence imaging of mitochondria stained with MitoTracker Deep Red (MTDR). Parental MDA-MB-231 cells displayed strong mitochondrial staining, whereas Rho0 cells exhibited markedly diminished fluorescence, indicating extensive mitochondrial clearance.

D) Immunoblot analysis of mitochondrial proteins TOMM20 and VDAC1, and E) quantitative analysis of protein expression demonstrate the near-absence of outer membrane proteins TOMM20 and VDAC1 in Rho0 cells, further validating the depletion of mitochondria.

Statistical test used: for B) one-way ANOVA ; for E) Two-tailed T test * $p<0.05$, ** $p<0.01$, *** $p<0.001$

DOI: 10.11134/btp.4.2025.16

To further explore the impact of mitochondrial depletion on cell cycle progression, parental and Rho0 cells were stained with propidium iodide and analysed by flow cytometry at 24 h and 48 h. In parental cells, the majority of the population resided in S phase at both time points (44.6% at 24 h; 45.1% at 48 h), consistent with active DNA replication and robust proliferation. In contrast, Rho0 cells demonstrated a pronounced accumulation in G1 phase (56.3% at 24 h; 59.5% at 48 h), accompanied by a reduction in S-phase population (Fig 4 B). These observations suggest that mitochondrial depletion delays progression from G1 to S phase, further contributing to the reduced proliferative capacity observed in the xCELLigence assays.

Collectively, these data indicate that loss of mtDNA and functional mitochondria in MDA-MB-231 cells results in slower growth rates and G1 cell cycle arrest, highlighting the critical role of mitochondria in supporting proliferation and cell cycle progression in triple-negative breast cancer cells.

To assess whether mitochondrial DNA depletion affected cellular energy status, intracellular ATP levels were quantified at 24 h and 48 h. No significant differences in ATP content were observed between parental and Rho0 cells at either time point (Fig. 4 C), indicating preservation of cellular ATP levels despite mitochondrial dysfunction. Consistently, lactate production measured at 24 h and 48 h was largely comparable between parental and Rho0 cells, although a slight reduction was observed in Rho0 cells (Fig. 4 D). This decrease did not reach statistical significance.

DISCUSSION

Mitochondria are central regulators of cellular metabolism, energy production, and signaling, and their loss profoundly reshapes cellular physiology. In this study, we established a stable model of mitochondrial depletion in the triple-negative breast cancer (TNBC) cell line MDA-MB-231 by leveraging Parkin overexpression combined with repetitive CCCP treatment. This approach allowed us to induce controlled mitophagy and generate Rho0 cells with near-complete loss of mitochondrial DNA (mtDNA) and mitochondrial structural proteins [19]. The rationale behind using Parkin overexpression was to exploit a physiological quality control mechanism known as mitophagy, in which depolarized mitochondria are selectively recognized and removed through the PINK1–Parkin pathway [20]. By doing so, we avoided strong chemical or mutagenic agents, such as ethidium bromide or nucleoside analogues, which, while effective at depleting mtDNA, carry risks of off-target toxicity and nuclear DNA damage [3, 10].

Our results demonstrate that sustained Parkin-mediated mitophagy induced by repetitive CCCP treatment leads to a

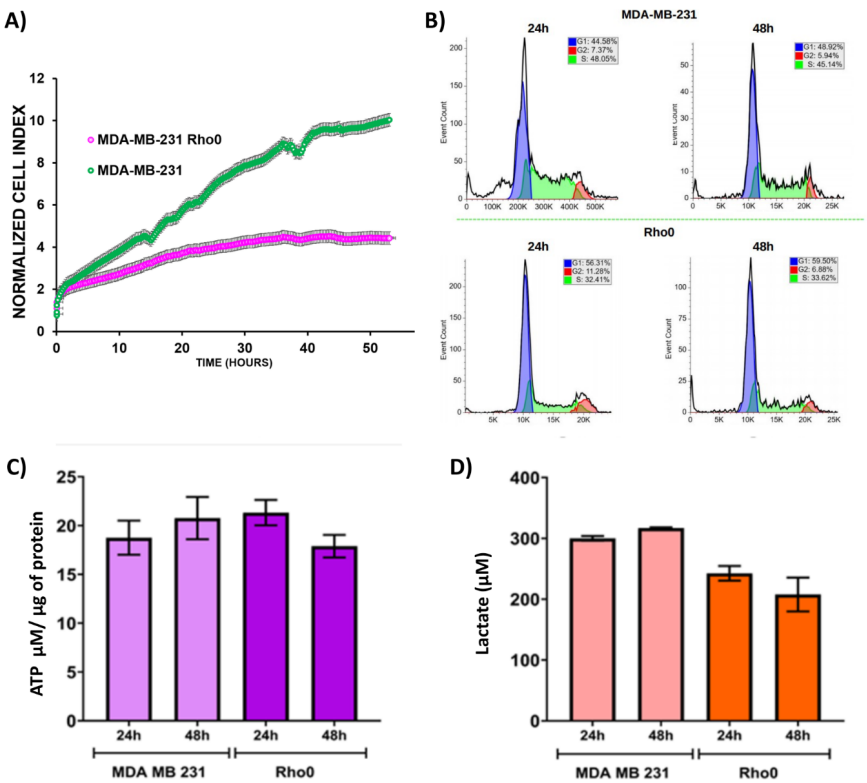

Figure 4. Impact of mitochondrial depletion on proliferation, cell cycle, and basal metabolism of MDA-MB-231 cells. A) Real-time monitoring of cell proliferation using the xCELLigence RTCA system. Parental cells (green) displayed a steady increase in cell index, whereas Rho0 cells (magenta), depleted of mitochondrial DNA, showed reduced proliferation, reaching a plateau at later time points. B) Flow cytometric analysis of cell cycle distribution at 24 h and 48 h. Parental cells remained in S phase, whereas Rho0 cells accumulated in G1, indicating delayed progression through the cell cycle. C) Cellular ATP levels measured at 24 h and 48 h. D) Lactate production at 24 h and 48 h. Data represent mean ± SEM of at least three independent experiments.

DOI: 10.11134/btp.4.2025.16

near-complete loss of mtDNA and mitochondrial membrane potential (MMP), accompanied by a profound reduction in mitochondrial protein levels.The sharp decline in mtDNA copy number, together with the almost undetectable MitoTracker Deep Red (MTDR) fluorescence, indicates a profound loss of mitochondrial membrane potential (MMP). These changes show that most mitochondria have also lost their respiratory capacity during enforced mitophagy. This pattern is consistent with advanced mitophagic clearance of damaged organelles. This distinguishes this system from conventional mitophagy studies, in which residual polarized mitochondria typically remain. Parkin overexpression likely facilitates this process by amplifying ubiquitination of outer membrane proteins and enhancing recognition by autophagosomes, accelerating mitochondrial turnover [13, 16]. These findings suggest that under conditions of strong mitophagic activation, cells undergo an extensive elimination of functionally competent organelles rather than simple fragmentation, remodelling or partial turnover. Despite the loss of mitochondrial function, the presence of faint TOMM20 and VDAC signals suggests that minimal outer membrane remnants remain. Such residual membranes are possibly structural fragments rather than metabolically active organelles. Similar observations have been reported in Rho0 cell models that have lost mtDNA and the proteins encoded by it, generated by chronic ethidium bromide exposure. There, only severely compromised, functionless mitochondrial structures, “mitochondrial ghosts”, persist without oxidative phosphorylation capacity [7, 22]. In our enforced mitophagy model, however, the depletion appears more immediate and complete, suggesting that active mitophagy eliminates functional mitochondria more efficiently than gradual chemical depletion.

The use of media supplemented with uridine and pyruvate is critical to maintain the ability of Rho0 cells to survive during mitochondrial clearance and maintain cellular viability [19, 23]. Without these supplements, mtDNA-depleted cells are unable to sustain DNA synthesis and rapidly arrest or die. The extra pyruvate provides a substrate for residual metabolic pathways, maintains redox balance and enables glycolytic flux, preventing catastrophic energy failure [7, 25, 26]. While the loss of mitochondrial function disrupts the de novo pyrimidine biosynthetic pathway, dihydroorotate dehydrogenase (DHODH) is particularly affected. DHODH, the mitochondrial enzyme that catalyzes the oxidation of dihydroorotate to orotate, requires an intact electron transport chain to transfer electrons to ubiquinone. Without this mitochondrial activity, cells are unable to synthesize uridine monophosphate (UMP) de novo and consequently rely on salvage pathways and external uridine sources to sustain nucleotide synthesis [27, 28]. Supplementation with uridine, therefore, enables Rho0 cells to maintain RNA and DNA synthesis for survival and proliferation in the absence of functional mitochondria.

Although uridine supplementation restored nucleotide availability, our findings showed that Rho0 MDA-MB-231 cells exhibited markedly reduced proliferation and cell-cycle progression. The shift in cell cycle dynamics was associated with the accumulation of Rho0 cells in the G1 phase and a reduction in the S-phase population, suggesting altered checkpoint regulation. This highlights that mitochondrial activity contributes to the cell cycle far beyond nucleotide production. These findings are also consistent with the critical role of mitochondria in coordinating biosynthetic and energetic demands necessary for cell cycle progression. The absence of fully functional mitochondria likely limits nucleotide and ATP availability for DNA synthesis, slowing the G1/S transition [29]. Interestingly, despite the severe mitochondrial loss, baseline ATP levels and lactate production remained largely unchanged compared with those of parental cells, suggesting metabolic adaptation [30, 31]. We expected a significant shift to glycolysis for energy production, which would typically decrease ATP and increase lactate, as reported for Rho0 cells. However, ATP and lactate levels remained comparable to controls. This indicates that the cells did switch almost entirely to glycolysis to compensate for the loss of mitochondrial ATP production. [3, 32]. The switch was efficient enough that total ATP levels were maintained, suggesting effective metabolic adaptation despite impaired mitochondrial function. Such metabolic plasticity is well documented in aggressive cancer cell types, particularly those with a preexisting glycolytic bias, such as MDA-MB-231 [32]. The cells’ ability to maintain energy balance despite the absence of mitochondria reflects their adaptability when oxidative phosphorylation is unavailable. This observation may reflect enhanced glycolytic flux or compensatory use of cytoplasmic substrates, a phenomenon observed in other Rho0 models [5, 33]. In the absence of mitochondrial respiration, Rho0 cells experience energetic and redox imbalances that limit ATP synthesis and perturb the NAD^+/NADH ratio, both of which are essential cofactors for DNA replication and chromatin-modifying enzymes [34, 35]. These energetic constraints likely slow replication fork progression and delay the G_1–S transition, leading to an accumulation of cells in early cell-cycle phases. Moreover, mitochondria contribute critical metabolites such as aspartate and formate, which feed into one-carbon metabolism and balance deoxyribonucleotide pools. Even when uridine compensates for pyrimidine deficiency, imbalances in dNTP ratios can cause replication stress, activate checkpoint kinases, and induce transient cell-cycle arrest [36, 37]. Interestingly, recent studies have revealed that uridine itself is not a completely inert supplement. Elevated intracellular uridine levels can influence redox balance, induce oxidative stress, and even modulate p53 signaling under specific conditions [38]. These effects may further contribute to altered checkpoint responses and reduced proliferation rates observed in Rho0 cells maintained in uridine-rich media. Thus, while uridine supplementation is essential to support survival of mitochondria-deficient cells, it cannot fully replicate the tightly coordinated metabolic environment maintained by functional mitochondria. Although it restores survival, it does not restore full proliferative competency in Rho0 cells. The persistent cell-cycle alterations observed reflect a convergence of nucleotide imbalance, energetic stress, and mitochondrial-to-nuclear communication pathways that remain unresolved despite external supplementation. This highlights the importance of carefully optimized culture conditions when studying Rho0 cells, as even physiologically regulated mitochondrial depletion imposes significant metabolic stress for the cells.

Our approach overcomes key limitations of conventional chemical or genetic depletion strategies and the Parkin-mediated system used in this study offers several clear advantages. Chemical methods, such as ethidium bromide or 2′,3′-dideox-

DOI: 10.11134/btp.4.2025.16

ycytidine (ddC), are effective but typically require prolonged exposure and carry inherent risks of mutagenesis. Similarly, nuclease-based strategies or dominant-negative *POLG* variants may produce incomplete mitochondrial clearance or off-target effects [11, 12]. In contrast, by harnessing the cell's natural quality-control pathway, Parkin overexpression enabled us to achieve gradual, reproducible mitochondrial depletion while maintaining nuclear genome integrity and overall cell viability. This approach yields homogeneous Rho0 populations, which are fully compatible with fluorescent reporters, metabolic profiling, and downstream mitochondrial transplantation for the generation of cybrid cells. This system is also a versatile platform for investigating mitochondrial retrograde signaling, bioenergetic adaptation, and combinatorial therapeutic studies in TNBCcells and can be adapted to other cells.

Despite the strengths of this study and the successful establishment of a mitophagy-driven workflow for generating Rho0 cells, several limitations should be acknowledged. First, although Parkin overexpression is a widely used tool to enhance mitophagy, Parkin is not endogenously upregulated in all cell types. Sustained or elevated Parkin levels may influence basal mitophagy rates and could affect non-mitochondrial processes, including general proteostasis. Similarly, while CCCP is a well-established mitochondrial uncoupler, it can exert off-target effects, including lysosomal pH disturbance and stress pathway activation. In this study, these issues were mitigated through careful optimisation of CCCP concentration and exposure intervals, as well as continuous viability monitoring; however, subtle off-target consequences cannot be entirely excluded. Second, although mtDNA depletion was validated by qPCR and mitochondrial membrane potential assays, residual mitochondrial fragments or "ghost mitochondria" may persist despite extensive clearance. These remnants may retain partial signalling or metabolic functions. Additional validation strategies, such as long-read mtDNA sequencing, TFAM immunostaining, or high-resolution mitochondrial imaging, would strengthen future studies aimed at confirming complete mtDNA loss. .Third, we used repetitive CCCP treatment in Parkin -overexpressing cells to trigger mitophagy by depolarizing mitochondria. While CCCP can sometimes cause ROS, we did not expect significant oxidative stress under our conditions; therefore, we did not measure ROS directly, as our focus was on selectively removing mitochondria, so the ROS induction during the depletion process cannot be excluded.Another constraint relates to the use of cancer cell lines, specifically MDA-MB-231. Cancer cells often display high metabolic plasticity and a reduced reliance on oxidative phosphorylation, making them more amenable to mitochondrial depletion strategies. In contrast, primary cells and differentiated tissues typically possess more robust mitochondrial networks and lower basal mitophagy, making them more resistant to induced mitophagy. Indeed, several studies report that primary human cells exhibit suppressed basal mitophagy and impaired clearance of damaged mitochondria [39], contributing to senescence and mitochondrial dysfunction [40]. These observations highlight the need for modified or cell-type-specific approaches when applying this workflow to primary or non-transformed cells. Extending the approach to additional cancer and non-cancer models will clarify whether the observed responses reflect generalizable features of mitophagy-driven mtDNA depletion or cell-line-specific adaptations. Future refinements such as inducible Parkin systems or alternative uncouplers with fewer off-target effects may further enhance temporal control and improve the precision of mitochondrial depletion strategies.

Looking ahead, several directions could further strengthen and broaden this workflow. Incorporating transcriptomic profiling and overall multi-omics approaches would allow us to better understand how cells rewire nuclear-mitochondrial communication and stress responses when mtDNA is lost. Another essential step will be to directly compare our mitophagy-driven Rho0 cells with those generated through ethidium bromide treatment or acute mitochondrial inhibition (e.g., Rotenone, Metformin). This will help clarify which cellular changes truly reflect mtDNA loss and which represent compensatory adaptations to different types of mitochondrial stress. Finally, applying this method to more cancer cell lines and, importantly, to primary or non-transformed cells will show how generalisable it is. This may also reveal cell-type-specific differences in mitochondrial resilience and quality-control pathways.

CONCLUSIONS

In conclusion, the controlled induction of mitophagy through Parkin overexpression and repetitive CCCP treatment results in the near-total removal of functional mitochondria, leading to severe mtDNA depletion and loss of membrane potential. Yet, the cells retain proliferative capacity by robust glycolytic adaptation and relying on uridine-supported nucleotide synthesis offering a physiologically relevant model to study mitochondrial biology, metabolic adaptation, and cancer cell plasticity. This highlights the mitochondrion's central role as a regulatory hub that links metabolism, biosynthesis, and control of proliferation. TNBC, including MDA-MB-231 cells, are known for their metabolic flexibility and reliance on both glycolysis and oxidative phosphorylation under different conditions [41]. By creating a controlled system in which mitochondria are selectively removed, we can investigate how TNBC cells compensate for mitochondrial bioenergetic loss, alter signaling pathways, and potentially develop resistance mechanisms to mitochondrial-targeting therapies. In this type of cancer, metabolic plasticity often underlies resistance to therapy and adaptation to microenvironmental stress. The study of Rho0 models, therefore, not only clarifies how cancer cells adapt to mitochondrial loss but also reveals potential vulnerabilities in their dependence on exogenous metabolites and salvage pathways, which can be exploited to study mechanisms of chemoresistance and inform future metabolic or synthetic-lethal therapeutic strategies.

Author Contributions

Conceptualization: A.B.; Methodology: A.D., A.B., B.K.; Investigation: A.D., B.K.; Writing: A.B., B.K.

FUNDING

The project was funded by the Ministry of Science and Higher Education of the Republic of Kazakhstan, AP23487802 to Agata N Burska

CONFLICTS OF INTEREST

The authors declare no competing interests.

DOI: 10.11134/btp.4.2025.16

DATA AVAILABILITY

All data supporting this study are available from the corresponding author upon reasonable request.

REFERENCES

1. Anderson S., Bankier A.T., Barrell B.G., de Bruijn M.H., Coulson A.R., Drouin J., et al. Sequence and organization of the human mitochondrial genome // Nature. – 1981. – Vol. 290. – P. 457–465.

2. Wallace D.C. Mitochondrial DNA mutations in disease and aging // Environ. Mol. Mutagen. – 2018. – Vol. 59. – P. 225–238.

3. King M.P., Attardi G. Human cells lacking mtDNA: Repopulation with exogenous mitochondria by complementation // Science. – 1989. – Vol. 246. – P. 500–503.

4. Ryan M.T., Hoogenraad N.J. Mitochondrial-nuclear communications // Annu. Rev. Biochem. – 2007. – Vol. 76. – P. 701–722.

5. Chandel N.S. Evolution of mitochondria as signaling organelles // Cell Metab. – 2015. – Vol. 22. – P. 204–206.

6. Wilkins H.M., Carl S.M., Swerdlow R.H. Cytoplasmic hybrid (cybrid) cell lines as models for mitochondrial biology // Methods Mol. Biol. – 2014. – Vol. 1137. – P. 123–139.

7. King M.P., Attardi G. Isolation of human cell lines lacking mitochondrial DNA // Methods Enzymol. – 1996. – Vol. 264. – P. 304–313.

8. Kennedy C.A., Tsaturian A., et al. Long-term effects of ethidium bromide on nuclear genome stability // J. Biol. Chem. – 2025. – Vol. 300. – P. 1015–1024.

9. Desjardins P., Frost B., et al. Mutagenic effects of ethidium bromide in human cells // Mutat. Res. – 1985. – Vol. 150. – P. 271–281.

10. Shokolenko I.N., Venediktova N., et al. Oxidative stress induces degradation of mitochondrial DNA // Nucleic Acids Res. – 2009. – Vol. 37. – P. 2539–2548.

11. Bacman S.R., Williams S.L., et al. Specific elimination of mutant mtDNA by mitochondrially targeted nucleases // Nat. Med. – 2013. – Vol. 19. – P. 1111–1117.

12. Spadafora D., Kozhukhar N., et al. *POLG* dominant-negative expression in mammalian cells // Hum. Mol. Genet. – 2016. – Vol. 25. – P. 4567–4576.

13. Geisler S., Holmström K.M., Skujat D., Fiesel F.C., Rothfuss O.C., Kahle P.J., et al. PINK1/Parkin-mediated mitophagy is dependent on VDAC1 and p62/SQSTM1 // Nat. Cell Biol. – 2010. – Vol. 12. – P. 119–131.

14. Pickrell A.M., Youle R.J. The roles of PINK1, Parkin, and mitochondrial fidelity in Parkinson's disease // Neuron. – 2015. – Vol. 85. – P. 257–273.

15. Youle R.J., Narendra D.P. Mechanisms of mitophagy // Nat. Rev. Mol. Cell Biol. – 2011. – Vol. 12. – P. 9–14.

16. Springer W., Kahle P.J. Regulation of PINK1/Parkin-mediated mitophagy // Autophagy. – 2011. – Vol. 7. – P. 116–118.

17. Lazarou M., Sliter D.A., Kane L.A., Sarraf S.A., Wang C., Burman J.L., et al. The ubiquitin kinase PINK1 recruits autophagy receptors to induce mitophagy // Nature. – 2015. – Vol. 524. – P. 309–314.

18. Correia-Melo C., Ichim G., Tait S., et al. Depletion of mitochondria in mammalian cells through enforced mitophagy // Nature Protocols. – 2017. – Vol. 12, No. 1. – P. 183-194.

19. Schmitz D.A., Oura S., Li L., Ding Y., Dahiya R., Ballard E., Pinzón-Arteaga C.A., Sakurai M., Okamura D., Yu L., Ly P., Wu J. Unraveling mitochondrial influence on mammalian pluripotency via enforced mitophagy // Cell. – 2025. – Vol. 188, No. 17. – P. 4773-4789.e22.

20. Narendra D.P., Youle R.J. The role of PINK1–Parkin in mitochondrial quality control // Nature Cell Biology. – 2024. – Vol. 26, No. 2. – P. 1639-1651.

21. Narendra D.P., Jin S.M., Tanaka A., Suen D.F., Gautier C.A., Shen J., Youle R.J. Parkin is recruited selectively to impaired mitochondria and promotes their autophagy // Journal of Cell Biology. – 2008. – Vol. 183, No. 5. – P. 795-803.

22. Kukat C., Wurm C.A., Spåhr H., Falkenberg M., Larrezon N.-G., Ståhlberg A. Super-resolution microscopy reveals that mammalian mitochondrial nucleoids have a uniform size and frequently contain a single copy of mtDNA // Proceedings of the National Academy of Sciences USA. – 2011. – Vol. 108, No. 33. – P. 13534-13539.

23. Mukherjee S., Das S., Das S., Gupta S., Hui S.P., Sengupta A., Ghosh A. Pyruvate plus uridine augments mitochondrial respiration and prevents cardiac hypertrophy in zebrafish and H9c2 cells // Journal of Cell Science. – 2025. – Vol. 138, No. 9. – jcs263653.

24. Bacman S.R., Williams S.L., Moraes C.T. Mitochondrial DNA depletion in cells using nucleoside analogs // Methods in Molecular Biology. – 2013. – Vol. 837. – P. 183-196.

25. Zhang J., Li Y., He D., et al. Mitochondrial dysfunction and nucleotide metabolism in cancer cells: Adaptive strategies for survival // Trends in Cell Biology. – 2023. – Vol. 33, No. 7. – P. 563-576.

26. Grasso D., Colleluori D., Masulli M., et al. Mitochondrial dysfunction and nucleotide metabolism in cancer // Trends in Cancer. – 2021. – Vol. 7, No. 9. – P. 777-790.

27. Adant I., Varga R., Favier J., et al. Uridine supplementation rescues mitochondrial translation defects and supports cell survival // Cell Metabolism. – 2022. – Vol. 34, No. 5. – P. 678-693.

28. Mandal S., Guptan P., Owusu-Ansah E., Banerjee U. Mitochondrial regulation of cell cycle progression during development as revealed by the tenured mutation in Drosophila. Dev. Cell. – 2005. – Vol. 9. – P. 843–854.

29. Buchet K., Godinot C. Functional F_1-ATPase essential in maintaining growth and membrane potential of human Rho0 cells. J. Biol. Chem. – 1998. – Vol. 273. – P. 22983–22989.

30. Bénard G., Rossignol R. Ultrastructure, bioenergetics and metabolism: a new role for mitochondria in cell cycle regulation. Biochim. Biophys. Acta. – 2008. – Vol. 1777. – P. 973–980.

31. Jones A.W., Yao Z., Vicencio J.M., et al. Glycolytic adaptation in mitochondrial DNA-depleted cells maintains bioenergetic homeostasis. Front. Cell Dev. Biol. – 2019. –

DOI: 10.11134/btp.4.2025.16

Vol. 7. – P. 282.

32. Vasan K., O'Connell J.T., Gonzalez Herrera K.N., et al. Mitochondrial functions in cancer cells: From the powerhouse to metabolic signaling hubs // Nature Reviews Cancer. – 2020. – Vol. 20. – P. 665-681.

33. Wallace D.C. Mitochondrial genetic medicine // Nature Genetics. – 2018. – Vol. 50. – P. 1642-1649.

34. Titov D.V., Brody J.R., Osheroff N., et al. Metabolic control of DNA replication through NAD^+-dependent enzymes // Nature Communications. – 2022. – Vol. 13. – Article 4561.

35. Cárdenas C., Smith B.D., Kalyanaraman B., et al. Mitochondrial redox regulation of the cell cycle // Frontiers in Cell and Developmental Biology. – 2023. – Vol. 11. – Article 1139487.

36. Birsoy K., Possemato R., Lorbeer F. K. et al. Respiratory chain dysfunction induces nucleotide imbalance and checkpoint activation // The EMBO Journal. – 2023. – Vol. 42. № 3. – P. e112233.

37. Molina-Castro S. E., Tahan S., Trefely S. et al. Mitochondrial metabolism coordinates dNTP pools and DNA replication fidelity // Cell Reports. – 2024. – Vol. 46. № 1. – Article 113776.

38. Li H., Wang X., Chen Y. et al. Uridine metabolism regulates p53 signaling and oxidative stress response // Experimental and Molecular Medicine. – 2025. – Vol. 57. № 3. – P. 214–227.

39. Kelly G., Kataura T., Panek J., Ma G., Salmonowicz H., Davis A., Kendall H., Brookes C., Ayine-Tora D.M., Banks P., Nelson G., Dobby L., Pitrez P.R., Booth L., Costello L., Richardson G.D., Lovat P., Przyborski S., Ferreira L., Greaves L., Szczepanowska K., von Zglinicki T., Miwa S., Brown M., Flagler M., Oblong J.E., Bascom C.C., Carroll B., Reynisson Jóhannes, Korolchuk V.I. Suppressed basal mitophagy drives cellular aging phenotypes that can be reversed by a p62-targeting small molecule // Developmental Cell. – 2024. – Vol. 59, No. 15. – P. 1924-1939.e7.

40. Chen Z., Berquez M., Luciani A. Mitochondria, mitophagy, and metabolic disease: towards assembling the puzzle // Cell Stress. – 2020. – Vol. 4, No. 6. – P. 147-150.

41. LeBleu V.S., O'Connell J.T., Gonzalez Herrera K.N., et al. PGC-1α mediates mitochondrial biogenesis and oxidative phosphorylation in TNBC // Cell Metabolism. – 2014. – Vol. 19, No. 5. – P. 812-823.